J. of Supercritical Fluids 48 (2009) 146–153

Contents lists available at ScienceDirect

The Journal of Supercritical Fluids

journal homepage: www.elsevier.com/locate/supflu

Solid catalyzed hydrogenation in a Si/glass microreactor using supercritical CO_2 as the reaction solvent

F. Trachsel [1], B. Tidona, S. Desportes, Ph. Rudolf von Rohr *

ETH Zurich, Institute of Process Engineering, Sonneggstrasse 3, Zurich CH-8092, Switzerland

ARTICLE INFO

Article history:
Received 4 June 2008
Received in revised form
29 September 2008
Accepted 30 September 2008

Keywords:
Microfluidic
Supercritical fluids
Glass/silicon microreactors
Catalytic hydrogenation
Flow visualization
Reaction performance

ABSTRACT

We present the use of supercritical CO_2 ($scCO_2$) as reaction solvent in a packed bed silicon/glass microreactor in case of the hydrogenation of cyclohexene as a model reaction. *In situ* phase studies in the continuous flow of the reaction mixture, hydrodynamic characterization and the influence of pressure and temperature on the reaction performance are discussed. The results are compared with the same reaction conducted in three phase gas–liquid–solid state and larger scale reactors using $scCO_2$ as reaction solvent. The phase study experiments show a single phase flow behavior at 136 bar and 25 °C for a 90:5:5 molar mixture of CO_2:C_6H_{10}:H_2. At 50 °C compositions up to 87.8:2.4:9.8 show single phase flow. The reaction performance increases with increasing temperature where pressure variations show no significant change. The comparison with larger scale systems indicates an increase of about one order of magnitude in space time yield in the presented microreactor.

1. Introduction

1.1. High pressure reactions in continuous flow microreactors

The advantage of high pressure microreactors compared to their macroscale counterparts is obvious. No excessive wall thickness of the reaction channel is needed for mechanical stability and the impact of hazardous failure is drastically reduced since only little quantities of material are involved. Until now only few studies discuss high pressure chemical reactions in continuous flow microreactors. The equipment such as precision high pressure pumps and back pressure regulators lead to high investment cost furthermore high pressure microfluidic connections are not yet standardized for chip-based microreactors. Mechanically stable microfluidic connections for high pressure and high temperature are still difficult to manufacture if different materials with different coefficients of thermal expansion are involved.

Most high pressure reactions in continuous flow microreactors are conducted in capillaries. This has several advantages such as the use of standard high pressure fluidic connections, inexpensive tubing and an adjustable reactor volume by the length of the capillary. The main drawback is the lack of optical transparency in metallic tubes and that the integration of different units such as mixing, heating and analysis is difficult to realize within one single capillary. A quartz capillary reactor is designed and used for oxidation studies in supercritical water by Maharrey and Miller [1]. The same authors performed online mass spectroscopy at the reactors outlet, designed as a nozzle [2]. A supercritical water microreaction setup made from Hastelloy capillaries is presented by Ikushima et al. [3]. A Silica fiber as microreactor is presented by Benito-Lopez et al. [4], where optical fibers are integrated via a cross-connection for UV/Vis monitoring of the reaction. A "step-by-step-rapid-mixing and heating" microfluidic system of Hastelloy capillaries for reactions in high pressure and high temperature water is designed by Kawanami et al. [5]. In conclusion the capillary-based microreactor studies point out the inexpensive capillaries, the rapid heating and quenching, the ease of handling high pressures and the low energy consumption compared to macroscale high pressure setups.

Chip-based microreactors follow the concept of the full integration of different units in one single chip. Precise micromachining possibilities enable the fabrication of μm-range features that is necessary for the design of passive mixing elements and flow control such as bubble formation. Glass or Si/glass as reactor material allows the optical access into the microfluidic reaction channel and is hereby advantageous. The more expensive fabrication compared to capillary reactors and the not standardized microfluidic connections may be accounted as drawbacks. Planar chip-type high pressure microreactors are rarely reported in literature. A

* Corresponding author. Tel.: +41 44 632 2488; fax: +41 44 632 1501.
E-mail address: vonrohr@ipe.mavt.ethz.ch (Ph. Rudolf von Rohr).
[1] Current address: DSM Nutritional Products, Basel CH-4002, Switzerland.

0896-8446/$ – see front matter © 2008 Elsevier B.V. All rights reserved.
doi:10.1016/j.supflu.2008.09.026

Table 1
High pressure reactions in continuous flow microreactors.

Reference	Experiment	Dimensions	Reactor material microfluidic connection	Range	Comments
Capillary-based microreactors					
[1,2]	Oxidation of acetic acid in scH_2O	d_h = 750 μm V_R = 148 μL	Quartz HPLC fittings	p = 280 bar T = 530 °C	Low energy required, online spectrometry
[3]	Acid catalyzed reactions in scH_2O	d_h = 250 μm V_R = 50 μL	Hastelloy C-276	p = 400 bar T = 400 °C	Possible production of 0.25 kg/d
[4]	Online UV/Vis spectroscopy	V_R = 3 μL	Silica HPLC fittings	p = 600 bar	Used conventional HPLC tools
[5]	C–C coupling reactions in water	d_h = 500 μm V_R = 3.5–1178 μL	Hastelloy C-276	p = 250 bar T = 250 °C	
Chip-based microreactors					
[6]	Monolithic stationary phase in microchannel	w = 80 μm h = 70 μm	Glass O-ring press fittings	p = 150 bar	No cleanroom facilities needed
[7]	Hydrogenation with $scCO_2$	d_h = 133 μm V_R = 8 μL	Glass	p = 90 bar $T \sim 60$ °C	High reaction productivity in 1 s
[8]	Carbamic acid formation in liquid CO_2	d_h = 42 μm V_R = 0.3 μL	Borosilicate glass Epoxy glued silica	p = 400 bar T = 100 °C	In-plane microfluidic connections
[9]	Esterfication with $scCO_2$	as [8]		p = 110 bar T = 100 °C	Significant rate enhancement
[10]	Hydrogenation of cyclohexene, LIF	d_h = 368 μm	Si/glass Soldered stainless steel tubing	p = 140 bar T = 80 °C	Packed bed microreactor

glass microreactor with press fittings is presented by Szekely and Freitag [6]. Kobayashi et al. [7] fed a premixed reaction mixture into a glass chip for the hydrogenation with $scCO_2$ as the reaction solvent. Glass microreactor chips were also used by Tiggelaar et al. [8] performing high pressure reaction with liquid CO_2. Benito-Lopez et al. [9] conducted the esterification reaction of phthalic anhydride with methanol in $scCO_2$ in a glass microreactor. Recently our laboratory performed a three phase hydrogenation in a Si/glass packed bed microreactor at high pressure [10]. Table 1 summarizes high pressure reactions in continuous flow microreactors.

1.2. Reactions with supercritical fluids as the reaction solvent

High pressure is used to enhance the reaction rate in chemical reactions. This is due to the thermodynamic pressure effect and in case of hydrogenations the increased solubility of hydrogen. The use of supercritical fluids in chemical reactions influences a variety of fluid characteristics which are beneficial for chemical reactions such as increased solubility, higher diffusivities than in liquids and the ease of product separation after the reaction to mention a few [11].

For our study the hydrogenation of cyclohexene using $scCO_2$ (T_c = 31 °C, p_c = 74 bar) as the reaction solvent as shown in Fig. 1 is used as a model reaction.

Hydrogenations belong to a reaction class of major importance since it is used in numerous synthesis pathways of common products and pharmaceuticals. Mass transfer limitations are often seen in these processes, which make them favorable to study at high pressure and with supercritical fluids (SCFs) as reaction solvents to overcome these limitations. Hitzler et al. [12] conducted the hydrogenation of cyclohexene in $scCO_2$ at pressures of 120–140 bar and catalyst bed temperature up to 340 °C in a 5 and 10 mL tube reactor. High conversion up to 99.8% is reported. Arunajatesan et al. [13] performed the same reaction at 136 bar and 70 °C in a 2.8 mL fixed bed reactor. They measured a conversion of 80% and an effective heat dissipation by the supercritical reactions mixture. Hot spots during the exothermic hydrogenation of cyclohexene in the packed bed were prevented.

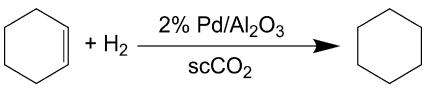

Fig. 1. Hydrogenation of cyclohexene.

In this study we focus on the reaction performance in a packed bed Si/glass microreactor using $scCO_2$ as the reaction solvent. Mixing of the reactants is realized on chip. The supercritical reaction mixture is observed by *in situ* phase studies. The observation of phase behavior for supercritical reaction studies is crucial. A change from a multiphase system to a single phase has significant influence on the heat and mass transfer behavior of the reaction. Therefore insight in the phase behavior of the reaction mixture at the operating conditions is needed to draw conclusions of the reaction performance. Since the presented Si/glass microreactor is optically accessible through the glass side, the phase studies can be conducted *in situ*. We decided for a Si/glass microreactor chip because of its advantages over capillary and glass chip-based designs. Microfabrication allows us to generate precise flow distribution and mixing features in the range of tens of μm. This is not possible in capillary reactors. Silicon as a reactor material provides high mechanical strength, chemical inertness and a high thermal conductivity providing a uniform temperature distribution on the chip. The optical access through the glass into the reaction channel is crucial for phase and flow studies.

2. Materials and methods

2.1. Microreactor design

The Si/glass microreactors are fabricated using standard photolithography, dry etching and anodic bonding techniques. The high pressure microfluidic connections are realized by soldering stainless steel capillaries directly onto the chip similar to the technique used in [14]. The detailed fabrication process and the high pressure testing of the chip are reported elsewhere [10]. The rectangular channel dimensions in the main section were 400 μm in width and 300 μm in depth respectively (d_h = 343 μm). These dimensions were chosen for a practicable handling of the particles and flow rates and the mechanical stability of the device. Furthermore the channel length provides the fluid to heat up to the set temperature for isothermal reaction conditions. The microreactor design as

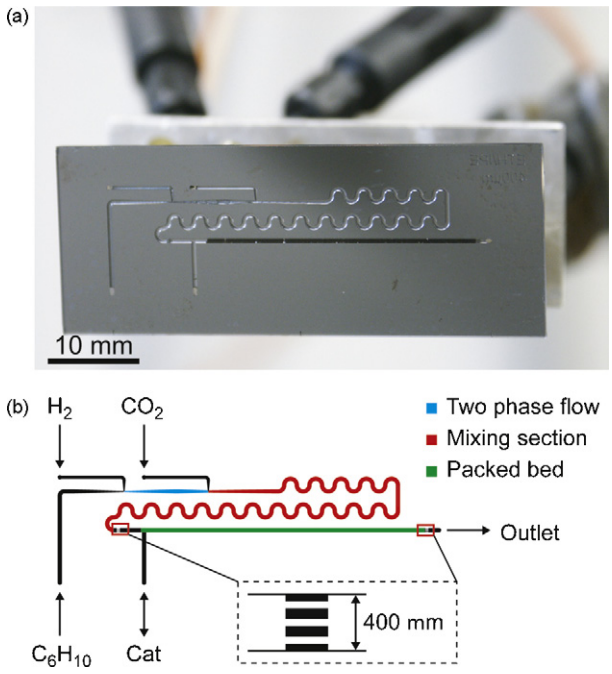

Fig. 2. Microreactor design. (a) Photograph of the Si/glass microreactor. (b) Schematic of the channel design.

shown in Fig. 2 consists of three inlets for the reactants, a meandering mixing section, a packed bed and a common outlet. The inlets were designed to primarily generate a stable segmented gas–liquid flow of C_6H_{10} and H_2, which is then dissolved by a side inflow of $scCO_2$. The 64.6 mm long mixing section provides the reactants to mix and generate a single phase reaction mixture. The meandering shape of the channel enhances mass transfer in the radial direction, when hydrogen bubbles are present [15]. The catalyst particles were inserted via a side channel into the microreactor forming a packed bed of a maximum length of 26.5 mm. Micromachined sieves at the entrance and exit of the packed bed define the length of the packed bed as described in [16].

2.2. Experimental setup

A versatile high pressure experimental setup for continuous operation as shown in Fig. 3 is used for the experiments. The setup allows the individual adjustment of the liquid and gas flow rates and of the system pressure. Stainless steel and polyetheretherketone (PEEK) capillaries (o.d. = 1.56 mm, i.d. = 0.5 mm) were used as tubing. High pressure PEEK connections (Upchurch Scientific) provide a leak tight connection of the microreactor to the setup. CO_2 and C_6H_{10} are fed in liquid phase by two water cooled high pressure syringe pumps (260D, ISCO). Hydrogen flow is controlled by a high pressure mass flow controller (F-230M, Bronkhorst). The pressure in the microreactor is controlled by an automated needle valve back pressure regulator (BP-1580-81, Jasco). The microreactor is placed in an oil bath for reactions at elevated temperatures.

Standard reaction conditions were 136 bar and 70 °C with flow rates of the reactants of $\dot{V}^*(CO_2) = 200\,\mu L/min$ (136 bar, 18 °C), $\dot{V}^*(C_6H_{10}) = 23\,\mu L/min$ (136 bar, 18 °C) and $\dot{V}^*(H_2) = 5.6$ sccm. The ratio of the flow rates corresponds to a molar ratio of $CO_2:C_6H_{10}:H_2 = 90:5:5$. The reaction performance is analyzed within temperature and pressure ranges from 40 to 70 °C and 80–150 bar respectively. For phase studies the $C_6H_{10}:H_2$ molar ratio is changed from 1:1 up to 1:4 to show the increase of hydrogen solubility in $scCO_2$. Samples are collected in a sample vial after the back pressure regulator. The vial is cooled in an ice water bath and the product is diluted in toluene to dissolve the product for GC analysis. The conversion is analyzed offline by GC–MS. The three highest conversion values at steady state conditions are averaged to calculate the maximum reaction rates. No side products are detected by GC–MS. The cyclohexene conversion is calculated from the chromatograms, where linearity between peak area and concentration is checked in the range of used conditions.

2.3. Optical measurements

The microreactor is placed on an inverse microscope (Axiovert 200, Zeiss) and illuminated with a triggered flash lamp. Images were taken with a CCD camera (1376 × 1040 pixel^2). With a 5× objective (NA = 0.12) the field of view (FOV) is 1.78 × 1.34 mm^2. For one experiment 200 pictures were taken at 10 Hz with an exposure

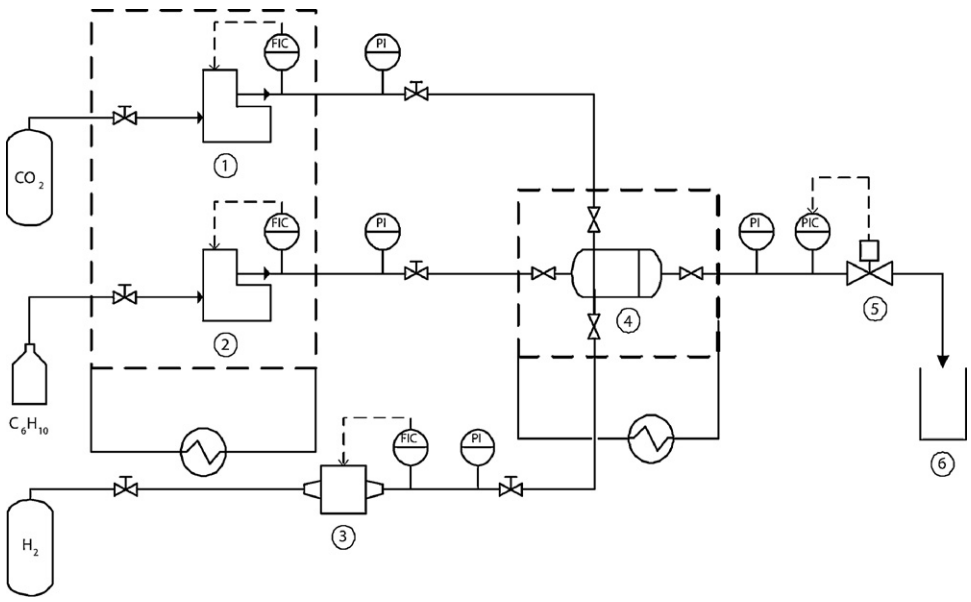

Fig. 3. Scheme of experimental setup. (1,2) Cooled high pressure syringe pumps. (3) Hydrogen mass flow controller. (4) Packed bed microreactor. (5) Back pressure regulator. (6) Sample vial.

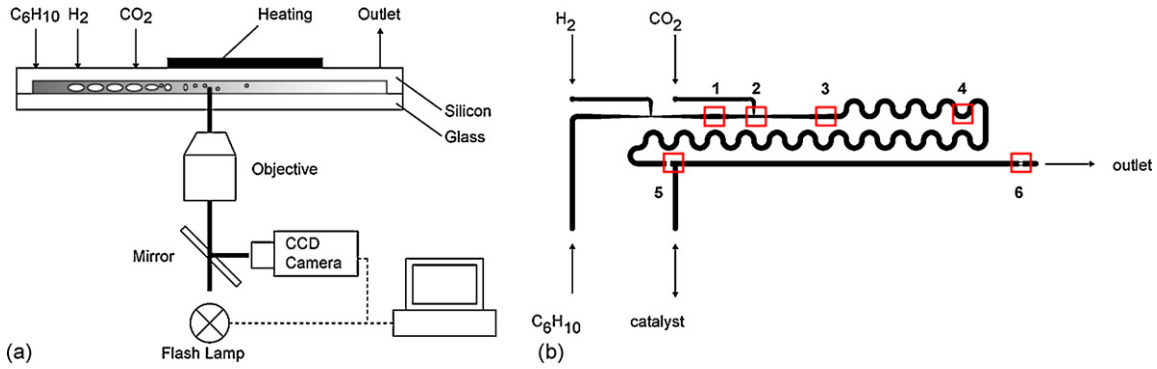

Fig. 4. (a) Experimental setup for *in situ* phase studies. (b) Measurement points for phase behavior analysis.

time of 100 μs. For temperature control a resistive heater foil and a resistance thermometer are placed on top of the microreactor. A DC controller regulates the temperature. A scheme of the configuration is seen in Fig. 4(a). This method of image acquisition has some drawbacks as the light reflection from the concave channel bottom and light scattering at phase boundaries, compared to fluorescence microscopy. But the main advantage of the possibility to observe the pure reaction mixture without the addition of dye prevails, since the influence of the large molecules of fluorescent dyes on the phase behavior is not known. Fig. 4(b) shows the location of the different measurement points.

2.4. Chemicals

Hydrogen and CO_2 (Pangas) were used as supplied with a purity of 99.999% and 99.995% respectively. Cyclohexene was purified by distilling at 80 °C adding iron chloride. The peroxides which have been indicated as catalyst poison [13] were reduced by this method from 2 mg(H_2O_2)/L to a not detectable amount using a colorimetric peroxide test (Merckoquant, Merck). As catalyst 2 wt% Pd/Al_2O_3 (Johnson Matthey) particles were used. After sieving a mean diameter of x_{50} = 115 μm was achieved and the particles were inserted into the microreactor applying vacuum at the outlet. The catalyst weight in the range of 0.5–1 mg was determined by measuring the weight of the dried empty and filled microreactor. For each experiment fresh catalyst was used and activated for 90 min at 70 °C with a hydrogen flow of 5 sccm at 20 bar.

3. Results and discussion

3.1. Phase studies

Following downstream direction the fluids undergo different flow regime and phase changes depending on the location of fluid feed and the microchannel design. For all analyzed conditions a general behavior can be observed. At measurement position (1) (see Fig. 4(b)) a segmented gas–liquid flow of H_2 and liquid C_6H_{10} is seen. The gas introduction via a narrow side channel provides a stable formation of gas bubbles and liquid slugs. The gas bubbles reduce and increase size in the subsequent section with the broadening and reducing channel width. At position (2) dense CO_2 is introduced from the side into the segmented gas–liquid flow. The superficial velocities of the merging stream at the CO_2 inlet (p = 136 bar, T = 24 °C, 90:5:5) are $v(C_6H_{10}) = 0.0053$ m/s, $v(H_2) = 0.0096$ m/s and $v(CO_2) = 0.088$ m/s. These large velocity gradients between CO_2 and the passing flow of hydrogen and C_6H_{10} lead to a break up of the well defined segmented flow pattern and a chaotic mixing of the compounds. H_2 bubbles and C_6H_{10} slugs are split into small fractions and the reactants start to solubilize in CO_2. Position (3) defines the beginning of the meandering mixing section. It is located 6.6 mm (=$26x/d_h$) downstream the CO_2 inlet. A bubbly flow of H_2 in a liquid mixture of CO_2 and C_6H_{10} is observed. In the meandering mixing section (4) the hydrogen continuously diffuses into the reaction mixture which itself is further mixed. At the entrance of the packed bed (5) the fluid passes the sieve with channel widths of 50 μm. Due to the reaction in the packed bed the concentrations in the mixture change and at the outlet (6) it has a different composition. As hydrogen is used during reaction the miscibility of the reaction mixture is increased, since lower hydrogen content increases the miscibility of the ternary reaction mixture [12].

In Fig. 5 the influence on temperature and C_6H_{10}:H_2 ratio on the phase behavior at different channel locations is seen. The pressure is fixed at p = 136 bar. Temperatures were 24 and 50 °C. The substrate to hydrogen molar ratios were 1:1, 1:2 and 1:4, where the mass flow rate of CO_2 was set constant at 200 μL/min (136 bar, 18 °C). From theses pictures a qualitative analysis of the phase behavior is described for the different locations.

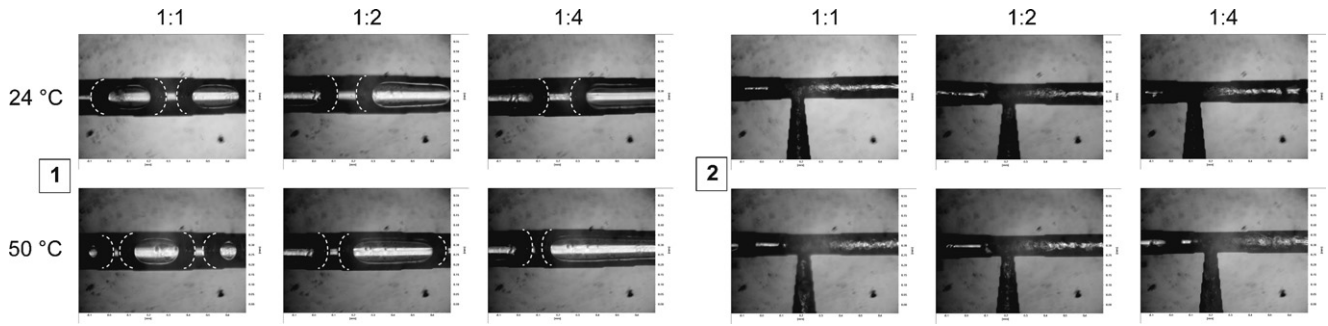

Fig. 5. Typical snapshot images of the phase behavior of the reaction mixture in the microreactor at the position 1 and position 2. Gas–liquid phase boundaries are indicated by dotted lines for better visibility.

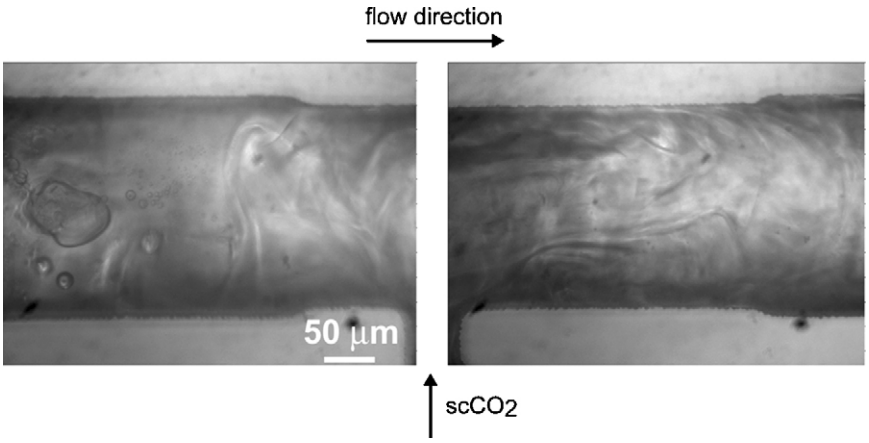

Fig. 6. Micrographs of the reaction mixture in the microfluidic channel using a 20× objective before and after the $scCO_2$ injection (position 2) at 136 bar and 50 °C. The substrate to hydrogen ratio was 1:2.

In Fig. 5 a stable segmented gas–liquid flow is observed at position (1). The influence of temperature on segmented gas–liquid flow is manly reflected in the decreasing slug length of C_6H_{10} and increasing bubble length of H_2 at constant C_6H_{10}:H_2 ratio. With decreasing C_6H_{10}:H_2 ratio the bubble length increases exceeding the FOV of the measurement section due to the higher gas flow rate of hydrogen.

At position (2) the break up of the segmented flow by CO_2 is difficult to characterize (Fig. 5). The CO_2 changes from liquid to supercritical state from 24 to 50 °C. In terms of flow pattern no significant change with temperature can be seen. By decreasing the C_6H_{10}:H_2 ratio coalesced hydrogen bubbles appear again earlier after the injection of CO_2. Fig. 6 shows in more detail how the two phase flow of H_2 and C_6H_{10} breaks up by the $scCO_2$ side inlet. As before the CO_2 inlet H_2 bubbles are seen, all H_2 is dissolved afterwards at the corresponding operating conditions.

In Fig. 7 hydrogen bubble coalescence appears in downstream position (3) of CO_2 injection. At 24 °C coalesced bubbles occur and form a bubbly flow pattern. A change from 24 to 50 °C results in the total solution of hydrogen in the reaction mixture. With increasing hydrogen content more and larger bubbles are present at 24 °C. At 50 °C for all C_6H_{10}:H_2 ratios a single phase flow is observed.

At the position (4) the dissolving of H_2 in the reaction mixture proceeds (Fig. 7). Disappeared bubbles or decreased bubble sizes are observed at 24 °C compared to position (3). With decreasing C_6H_{10}:H_2 ratio more and larger bubbles are present. At 50 °C single phase flow is observed.

In Fig. 8 at the inlet to the packed bed, position (5), most hydrogen has been dissolved at 24 °C. At 1:2 and 1:4 small bubbles are visible. At 50 °C no change on the previously detected single phase flow is observed. The reaction mixture enters the reaction zone as a single phase at 136 bar and 50 °C for high hydrogen content such as 9.8 mol%.

In Fig. 8, regard to the position (6) at the reactors outlet only at 24 °C and a ratio of 1:4 H_2 bubbles are observed. In all other cases the hydrogen was entirely dissolved in the reaction mixture. The two effects of an enhanced mixing in the packed bed and the hydrogen consumption increase the homogeneity of the reaction mixture.

At 24 °C only at high H_2 content the mixture was not present in one single phase. This is due to the limited solubility of H_2 in the mixture but also due to the short residence time in the reactor. At 50 °C no H_2 bubbles can be detected at the entrance to the packed bed within the number of recorded images. This leads to the conclusion that the reactants are present in one single phase. At the outlet the reaction mixture contains CO_2, C_6H_{10}, C_6H_{12} and H_2 which is a quaternary mixture, but the critical points of C_6H_{10} (T_c = 287.3 °C) and C_6H_{12} (T_c = 280.3 °C) are relatively close together that the system can be considered as ternary mixture, which was modeled by Hitzler et al. [12] using Peng-Robinson equation of state. A single phase behavior of a 90:5:5 mixture at 120 bar and 50 °C can be derived from their results. Arunajatesan et al. [13] conducted phase studies in a high pressure view cell and suggested a homogeneous phase of a 30% converted reaction mixture at about 115 bar and 70 °C. In our experiments it is seen that high hydrogen contents can be dissolved in the reaction mixture using $scCO_2$ as the reaction solvent. This is not possible in case of a reaction mixture containing only C_6H_{10} and H2. Using an estimated Henry constant of H = 2648.5 bar (T = 50 °C, p = 136 bar) [17] H_2 would be soluble in C_6H_{10} in the extent of x = 0.05 mol H_2/mol

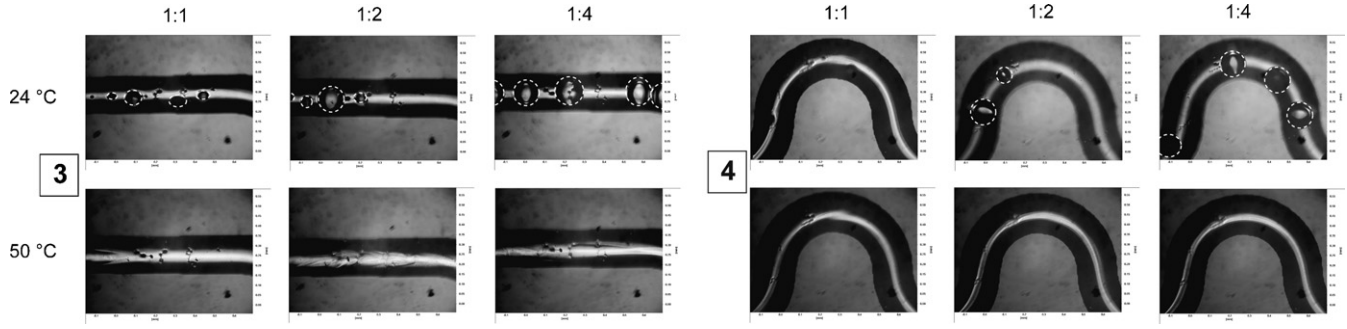

Fig. 7. Typical snapshot images of the phase behavior of the reaction mixture in the microreactor at the position 3 and position 4. Gas–liquid phase boundaries are indicated by dotted lines for better visibility.

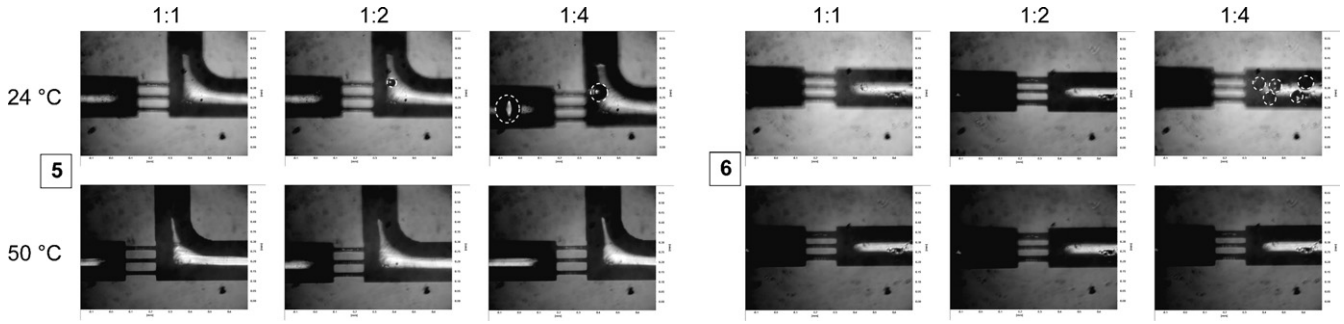

Fig. 8. Typical snapshot images of the phase behavior of the reaction mixture in the microreactor at the position 5 and position 6. Gas–liquid phase boundaries are indicated by dotted lines for better visibility.

C_6H_{10}. This low hydrogen solubility results in a two phase flow and often causes mass transfer limitations in three phase catalytic reactions.

3.2. Reaction performance

The reactions were conducted at constant flow rate of the reactants $V^*(CO_2) = 200\ \mu L/min$, $V^*(C_6H_{10}) = 23\ \mu L/min$ both at 136 bar and 18 °C (pump feed conditions) and $V^*(H_2) = 5.6$ sccm. This corresponds to a molar ratio of 90:5:5. To demonstrate the influence of operating conditions on the reaction performance temperature and pressure in the microreactor were varied in the range of $T = 40–70\ °C$ and $p = 80–150$ bar, respectively. At constant pressure of 136 bar it can be stated from the optical analysis that the reaction mixture is present in a single phase for the observed temperature range. The pressure variation was performed at 50 °C and pressures ranging from 80 to 150 bar. For pressures higher than 100 bar a single phase is present. At 80 bar a two phase flow of H_2 and $scCO_2/C_6H_{10}$ was observed.

The mean residence time through the packed bed with a measured porosity of 0.688 was calculated in the range of $t_{mean} = 0.17–0.5$ s depending on the temperature. Isothermal conditions of the microreactor were assumed because of the low Biot number in the order of $Bi = 1 \times 10^{-3}$, where Bi is defined as $L_c h/\lambda$. L_c is the characteristic length of the microreactor, h is the heat transfer coefficient from the microreactor to the environment and λ is the thermal conductivity of the microreactor material. Conversions observed were between 20 and 93%, depending on the catalyst loading and operating conditions. The performance of the microreactor is expressed by the converted moles of C_6H_{10} per time per mass of catalyst (Fig. 9).

In Fig. 9 the influence of temperature on the reaction rate is shown. An increase in reaction rate with increasing temperature is obvious due to Arrhenius law. The reaction mixture is in single phase for all experiments, even at subcritical temperatures of CO_2 as seen in the phase study. At isobaric conditions density, dynamic viscosity and thermal conductivity of the reaction solvent CO_2 decrease with increasing temperature, which leads to different observations. The kinematic viscosity, which has a big influence on mass transfer, changes only little in the range from 7.4×10^{-8} to $8.5 \times 10^{-8}\ m^2/s$. A decrease in thermal conductivity decreases the heat removal from the exothermic reaction. The maximum heat produced by the reaction is $Q^* = 3.84 \times 10^{-6}\ mol/s \times -118\ kJ/mol = -0.45$ W. In an earlier experiment a lumped heat transfer coefficient from the microreactor surface to the environment of about $h = 25\ W/m^2\ K$ was measured. The heat loss at the surface dominates therefore the heat generation of the reaction above a temperature difference of 13 K.

Fig. 10 shows the dependency of the reaction performance on pressure. No significant change in reaction rate can be observed with increasing pressure. Several effects have an important influence on the reaction rate by varying the pressure. First the density of the reaction mixture increases with higher pressure meaning the diffusion coefficient is lowered. If the reaction were diffusion controlled this leads to a decrease in reaction rate. Second the concentration or partial pressure of the involved compounds increase with increasing pressure. This would result in a higher reaction rate with increasing pressure. Additionally changing the density of the system changes the residence time in the microreactor.

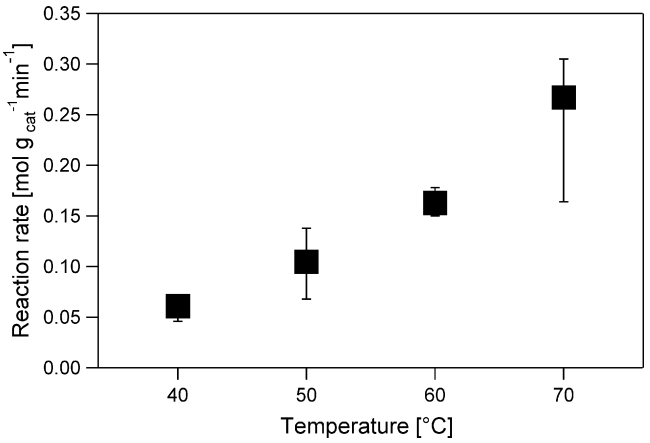

Fig. 9. Temperature vs. reaction rate at $p = 136$ bar. $V^*(CO_2) = 200\ \mu L/min$, $V^*(C_6H_{10}) = 23\ \mu L/min$ and $V^*(H_2) = 5.6$ sccm.

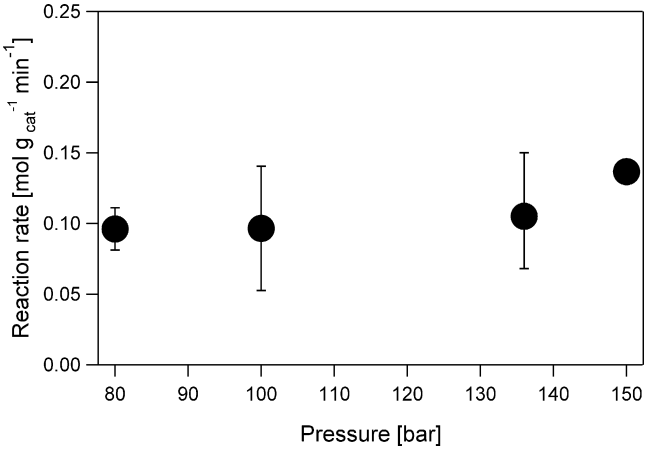

Fig. 10. Pressure vs. reaction rate at $T = 50$ °C. $V^*(CO_2) = 200\ \mu L/min$, $V^*(C_6H_{10}) = 23\ \mu L/min$ and $V^*(H_2) = 5.6$ sccm able.

Table 2
Space time yields for the solid catalyzed hydrogenation of cyclohexene in different reactors for gas–liquid (*) and single phase reactions with $scCO_2$ as reaction solvent.

Reference	Reactor volume	Conditions	Catalyst	Space time yield
[16]	3.75 μL	~25 °C, ~1 bar	1–5% Pt/Al_2O_3	7.1×10^3*
[10]	3.4 μL	71 °C, 51 bar	2% Pd/Al_2O_3	2.6×10^5*
[12]	5 mL	~340 °C, 120 bar	5% Pd/Deloxan	2.5×10^5
Present study	3.8 μL	70 °C, 136 bar	2% Pd/Al_2O_3	1.5×10^6

3.3. Comparison of reactor performance

The efficiency of the presented microreactor in terms of reaction performance is compared to other packed bed reactors at the μL- and mL-scale. As a measure we compare the space time yield ($kg_{product}/hm^3_{catalyst}$) for the hydrogenation of cyclohexene in the case of a three phase reaction and with $scCO_2$ as the reaction solvent. The increase of efficiency in different reactor systems is manifold. Applying high pressure increases the performance because it increases the hydrogen solubility. Using $scCO_2$ as reaction solvent also enhanced productivity since the mass transfer resistance from the gas to the liquid phase vanishes in single phase flow. The single phase behavior of the reaction mixture, confirmed by optical measurements, avoids the gas/liquid mass transfer resistance. The concentration of the hydrogen within the single phase is controlled by the flow rate applied not by the solubility of hydrogen within the reaction media since H_2 and CO_2 are fully miscible. The efficiency of the microreactor system is further increased by a good heat removal from the catalyst due to the higher heat capacity of the dense gas and the good thermal conductivity of silicon (150 W/m K). Table 2 lists space time yields for different systems found in literature. In case of a three phase reaction the influence of pressure leads to an increase of efficiency of one order of magnitude. The high pressure three phase microreactor has a performance in the same range than the 5 mL reactor at supercritical conditions. The large surface-to-volume ratio of the microreactor combined with the good thermal conductivity of Si leads to an increased heat removal from the exothermic reaction. The present study increases the efficiency by another order of magnitude compared to the larger reactor at supercritical conditions. This is attributed to the better heat removal, which can be realized in microreactors avoiding hot spots in the packed bed.

For the identification of possible external mass transfer limitation at the liquid–solid interface a quantitative analysis is difficult to conduct due to the lack of correlations to estimate the mass transfer coefficient in a microscale packed bed. Concerning the pore diffusion limitation the Weisz criterion [18] gives an indication of the limiting step. The analysis was performed for the experiments where the conversion was around 20%, at $p = 136$ bar and $T = 40$ °C. In this case, we assume a differential reactor. The bulk concentration of hydrogen is assumed to be the concentration at the surface of the particles. The molecular diffusion coefficient of hydrogen in $scCO_2$ is estimated at 1×10^{-8} m^2/s. This is the order of magnitude reported in different papers. This value is for sure underestimated, in experiments carried out by Ludemann and Chen [19] reported this value for $T = 253$ K and $p = 1000$ bar. Thus the Weisz criterion, at our reaction conditions, is below 0.1. This means that the internal mass transfer does not limit the reaction.

4. Conclusions

A chip-based Si/glass packed bed microreactor for reactions using $scCO_2$ as the reaction solvent has been presented. As a model reaction the hydrogenation of cyclohexene over Pd/Al_2O_3 catalyst is studied. All reactants are brought in contact, mix and react on the chip. *In situ* phase studies of the reaction mixture and the reaction performance were discussed. The phase studies confirmed a single phase reaction mixture at 25 and 50 °C during isobaric reaction conditions of 136 bar. The reaction performance increased with temperature whereas with increasing pressure no significant increase was observed. A comparison of the reactor performance in terms of space time yield with different reactor systems for the same model reaction is presented. The results indicate that high pressure microreactors are favorable for exothermic reactions because of the good heat removal due to the small reactor length scales. The space time yield is one order of magnitude greater than earlier reported values. Nevertheless, the translation to commercial scale throughput in microreactors still needs further investigations. Especially, the manifold design hence the equal distribution of fluid into numerous parallel microchannels must be addressed.

This study shows the feasibility of high pressure Si/glass microreactors for reactions using $scCO_2$ as the reaction solvent. The concept of an integrated high pressure microreactor chip is used for future *in situ* spectroscopic measurements. Further studies will investigate *in situ* spectroscopic analysis methods as UV/Vis and Raman which will provide deeper insights in high pressure heterogeneous reactions involving supercritical fluids.

Acknowledgements

This work was supported by the ETH Research Grant TH-32/05-2 and the Emil Barell Foundation.

References

[1] S.P. Maharrey, D.R. Miller, Quartz capillary microreactor for studies of oxidation in supercritical water, AICHE Journal 47 (5) (2001) 1203–1211.
[2] S.P. Maharrey, D.R. Miller, A direct sampling mass spectrometer investigation of oxidation mechanisms for acetic acid in supercritical water, Journal of Physical Chemistry A 105 (24) (2001) 5860–5867.
[3] Y. Ikushima, K. Hatakeda, M. Sato, O. Sato, M. Arai, Innovation in a chemical reaction process using a supercritical water microreaction system: environmentally friendly production of epsilon-caprolactam, Chemical Communications 19 (2002) 2208–2209.
[4] F. Benito-Lopez, W. Verboom, M. Kakuta, J.G.E. Gardeniers, R.J.M. Egberink, E.R. Oosterbroek, A. Van den Berg, D.N. Reinhoudt, Optical fiber-based online UV/Vis spectroscopic monitoring of chemical reaction kinetics under high pressure in a capillary microreactor, Chemical Communications 22 (2005) 2857–2859.
[5] H. Kawanami, K. Matsushima, M. Sato, Y. Ikushima, Rapid and highly selective copper-free Sonogashira coupling in high-pressure, high-temperature water in a microfluidic system, Angewandte Chemie-International Edition 46 (27) (2007) 5129–5132.
[6] L. Szekely, R. Freitag, Fabrication of a versatile microanalytical system without need for clean room condition, Analytica Chimica Acta 512 (1) (2004) 39–47.
[7] J. Kobayashi, Y. Mori, S. Kobayashi, Hydrogenation reactions using $scCO_2$ as a solvent in microchannel reactors, Chemical Communications 20 (2005) 2567–2568.
[8] H.J.G.E. Gardeniers, R.M. Tiggelaar, F. Benito-Lopez, D.C. Hermes, H. Rathgen, R.J.M. Egberink, F.G. Mugele, D.N. Reinhoudt, A. Van den Berg, W. Verboom, Fabrication, mechanical testing and application of high-pressure glass microreactor chip, Chemical Engineering Journal 131 (1–3) (2007) 163–170.
[9] F. Benito-Lopez, R.M. Tiggelaar, K. Salbut, J. Huskens, R.J.M. Egberink, D.N. Reinhoudt, H.J.G.E. Gardeniers, W. Verboom, Substantial rate enhancements of the esterification reaction of phthalic anhydride with methanol at high pressure and using supercritical CO_2 as a co-solvent in a glass microreactor, Lab on a Chip 7 (10) (2007) 1345–1351.
[10] F. Trachsel, C. Hutter, Ph. Rudolf von Rohr, Transparent Silicon/glass microreactor for high-pressure and high-temperature reactions, Chemical Engineering Journal 135 (Suppl. 1) (2008) S309–S316.
[11] A. Baiker, Supercritical fluids in heterogeneous catalysis, Chemical Reviews 99 (2) (1999) 453–473.
[12] M.G. Hitzler, F.R. Smail, S.K. Ross, M. Poliakoff, Selective catalytic hydrogenation of organic compounds in supercritical fluids as a continuous process, Organic Process Research & Development 2 (3) (1998) 137–146.
[13] V. Arunajatesan, B. Subramaniam, K.W. Hutchenson, F.E. Herkes, Fixed-bed hydrogenation of organic compounds in supercritical carbon dioxide, Chemical Engineering Science 56 (4) (2001) 1363–1369.

[14] E.R. Murphy, T. Inoue, H.R. Sahoo, N. Zaborenko, K.F. Jensen, Solder-based chip-to-tube and chip-to-chip packaging for microfluidic devices, Lab on a Chip 7 (10) (2007) 1309–1314.
[15] A. Gunther, S.A. Khan, M. Thalmann, F. Trachsel, K.F. Jensen, Transport and reaction in microscale segmented gas–liquid flow, Lab on a Chip 4 (4) (2004) 278–286.
[16] M.W. Losey, M.A. Schmidt, K.F. Jensen, Microfabricated multiphase packed-bed reactors: characterization of mass transfer and reactions, Industrial & Engineering Chemistry Research 40 (12) (2001) 2555–2562.
[17] M.J. Herskowitz, W. Wisniak, L. Skladman, Hydrogen solubility in organic liquids, Journal of Chemical and Engineering Data 28 (2) (1983) 164–166.
[18] O. Levenspiel, Chemical Reaction Engineering, vol. XVI, third ed., Wiley, New York, 1999, p. 388.
[19] H.D. Ludemann, L.P. Chen, Transport properties of supercritical fluids and their binary mixtures, Journal of Physics-Condensed Matter 14 (44) (2002) 11453–11462.